High Capacity Dual-Polarization THz-Wireless Transmission in the 300 GHz Band using a Broadband Orthomode Transducer

Oliver Stiewe[#], Thomas Merkle[*], Robert Elschner[#], Joachim Hoppe[*], Colja Schubert[#], Ronald Freund[#]
[#]Fraunhofer Institute for Telecommunications, Heinrich Hertz Institute, HHI, Germany
[*]Fraunhofer Institute for Applied Solid State Physics, IAF, Germany
{oliver.stiewe@hhi, thomas.merkle@iaf, robert.elschner@hhi, joachim.hoppe@iaf}.fraunhofer.de
{colja.schubert@hhi, ronald.freund@hhi}.fraunhofer.de

***Abstract* — We report on the broadband, dual-polarized THz-wireless transmission with >100 Gb/s net data rate in the 300 GHz band, employing a new broadband orthomode transducer. The orthomode transducer is realized by a new microstrip probe-fed circular waveguide transition. It omits the use of hybrids for the commonly used balanced 4-port excitation and, for that reason, is more suitable for a planar active integration with transceiver MMICs. The characterization of the orthomode transducer in back-to-back configuration shows very low losses of less than 1.5 dB per transition over a bandwidth of more than 40 GHz with a total back-to-back cross polarization better than 25 dB. Constellation diagrams and signal spectra from the dual-polarized wireless transmission experiments are compared to single-polarized transmission, showing only small degradations due to cross-polarization effects. The paper demonstrates that this simplified polarization multiplexer is a potential candidate for use in a wireless extender of a coherent fiber-optical transmission system.**

***Keywords* — Terahertz wireless communications, 6G communications, Polarization multiplexer, Orthomode transducer, Digital signal processing,**

I. Introduction

THz-wireless communications is widely regarded as one of the key technologies for future 6G networks [1], supporting the requirement of the massive increase in the wireless data rate and lowering network latencies e.g., by advanced fiber-optical and wireless integration on the physical layer [2]. This is mainly because a large contiguous bandwidth is available for THz-wireless communication e.g., between 252 GHz – 320 GHz, which is suitable for high capacity transmission beyond 100 Gb/s using single-carrier modulation with high symbol rates [3]. Recently, this is also addressed by first IEEE standards [4]. In order to further increase the link capacity, polarization multiplexed, i.e., dual-polarized transmission can be used [3],[5]. Instead of using the polarization domain for the enabling a full-duplex operation, very high gain antennas are used to exploit the spatial domain for this purpose.

In this work, we report on the use of a new broadband low-loss orthomode transducer (OMT) that enables a planar active integration of the polarization-multiplexing function with transceiver MMICs in the 300 GHz band. There is a number of solutions for OMTs that require rather complex 3D-machining for fabrication e.g., the T-junction OMTs [6], the Boifot OMTs [7], or the turnstile junction OMTs [8]. Recently, multi-layer 2.5D-silicon micromachining has been demonstrated as an interesting fabrication solution, as well as additive 3D fabrication. In contrast, planar solutions using microstrip-probe fed circular waveguide junctions have been mostly used at lower frequencies so far [9] since their feeding network may degrade the insertion loss performance [10] and the coupling between the probes degrades the cross-polarization performance. The planar microstrip probe fed OMT of this work circumvents the problem of insertion losses in the feed networks by asymmetrically feeding the back-shorted circular waveguide, similar to a rectangular waveguide, which omits the feeding networks. The cross polarization performance is improved by probe and backshort optimization.

It is of high interest to test if the proposed new planar OMT solution is suitable for high speed dual-polarized transmission and can be applied at the 300 GHz band. For this purpose, the OMT was used as part of a dual-polarized over-the-air transmission system experiment with a net data rate of up to 100 Gb/s. The results are compared to a single-polarization measurement in order to discuss the impact of the measured OMT characteristics, i.e., first of all cross-polarization, but also in order to verify the performance in the presence of residual spike-like resonances due to excitation of higher order circular waveguide modes and misalignment, often seen in OMTs [11].

II. Broadband Planar Orthomode Transducer

A. Concept, Design and Implementation

The OMT was designed to connect two WR-3 rectangular waveguide (RWG) ports that support the two separated polarizations as a single TE10 mode each, with a circular

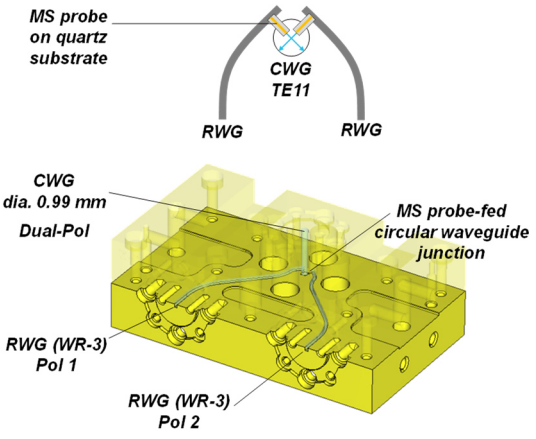

Figure 1: Functional block diagram and CAD model of the planar OMT.

waveguide (CWG) port. The CWG transmission line section is perpendicular to the plane of the two RWG transmission line sections, as depicted in the CAD model of the OMT in Figure 1. The CWG section supports two polarizations orthogonal to each other in the TE11 mode. The diameter of the CWG interface is 0.99 mm covering the frequency band from 220 – 330 GHz. Although not standardized, this is a commonly used diameter for CWG components in this frequency band. The selected diameter means that the CWG flange can support higher order modes, if excited, most critical the TM01 mode with a lower cut-off frequency of 231 GHz.

The transition between the rectangular waveguide modes and the circular waveguide modes is accomplished by two microstrip probes, which are implemented on a 50 µm thick quartz substrate. The two probes are oriented perpendicular to each other corresponding to the two polarizations in the CWG section, which, when connected to a CWG horn antenna, represent the orientation of the radiated orthogonal polarizations. The functional block diagram of Figure 1 also indicates that the microstrip probe is actually composed of two waveguide transitions, the RWG→MS transition and the MS→CWG transition. In an active integrated planar version, the RWG→MS transition can be replaced by a MMIC→MS transition, which reduces the overall system losses and enables a fully planar integration of MMICs and CWG probes.

B. *Component Characterization*

Four planar OMTs were fabricated for testing their modal behavior and if the assembly leads to reproducible results. The OMTs were connected by a 25 mm long CWG transmission line section (CWG diameter 0.99 mm) in a back-to-back configuration as shown in the photograph and the block diagram of Figure 2. For this reason, the measured S-parameters represent the behavior of two cascaded OMTs. Since the 25 mm CWG line supports higher order modes, any excitation of higher order modes by mismatch or the MS→CWG transition leads to spike-like resonances [11] that may be detrimental to the performance of a wireless data link.

Figure 3 summarizes the measured S-parameters (back-2-back) for combinations of the four fabricated OMTs connected to each other. Since the S-parameters are nearly

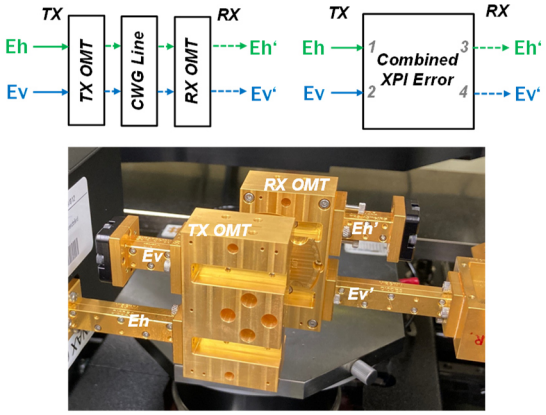

Figure 2: S-parameter measurement setup of the fabricated 300 GHz OMT in back-2-back configuration.

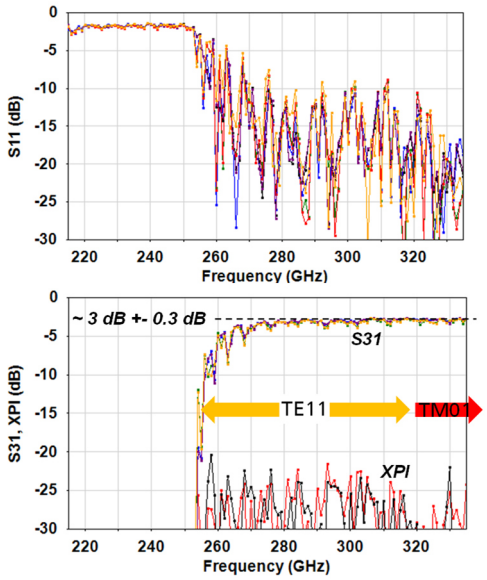

Figure 3: Measured S-parameters of four fabricated OMTs connected in back-2-back configuration. Different colors indicate different OMTs connected in back-2-back configuration.

identical with respect to the input reflection coefficient (Sii) as well as the losses (S31) and the cross polarization (XPI), the measurements indicate an excellent reproducibility of the fabrication and assembly process. The measured cross polarization performance was approximately 23 dB. Assuming an additive rotational error, the cross polarization of a single OMT is approximately 30 dB. The measured insertion loss was approximately 3 dB which means that the single transition had an insertion loss of 1.5 dB.

III. High Capacity Dual-Polarization THz-Wireless Transmission

A. *Experimental Setup*

Figure 4 shows the schematic drawing of the experimental setup for P2P measurements with dual Tx and Rx modules including the OMT. A sine wave generator provides the required clock signal for the arbitrary waveform generator (AWG) (3dB BW = 15 GHz). Two PLLs provide the external local oscillator (LO) signals for up- and down-mixing at the Tx and Rx frontends. The real-time oscilloscope (RTO) (3dB BW = 20 GHz) is connected to the AWG sine wave generator via a 10 MHz reference line. In-phase and quadrature (IQ) signals for the Tx frontends are generated by an AWG from single and dual polarization 4QAM waveforms with a sample rate of 84 GS/s. The IF side of the Tx frontends is connected directly to the AWG via coaxial cables. The RF in- and outputs of Rx and Tx are connected to the OMT via WR-3 waveguides. A carrier frequency of approx. 300 GHz is used. After 40 cm, the RF signal is received and amplified in the baseband with a gain of 20 dB. Amplification is necessary to get a suitable signal voltage for the analog-to-digital conversion at the RTO. The RTO samples the signal with a sample rate of 50 GS/s. At the end, offline digital signal processing is performed with blocks of at least 1,000,000 samples.

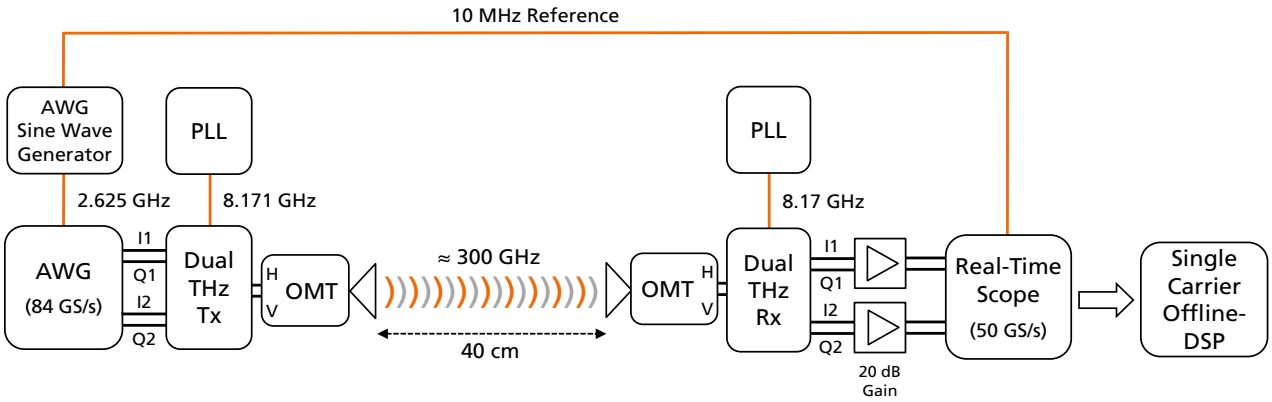

Figure 4: Schematic setup for dual polarization measurements (AWG: Arbitrary Waveform Generator, OMT: Orthomode Transducer, PLL: Phase Locked Loop).

A training-aided single-carrier DSP [12], originally used in high-capacity dual-polarization fiber-optical communications, serves as Tx and Rx DSP. It contains blocks for frontend corrections, training-aided frame synchronization, frequency offset estimation and channel estimation, and T/2-spaced frequency-domain equalization. This is followed by a carrier-phase estimation (CPE) using the blind phase search algorithm, and T-spaced adaptive equalization using a decision-directed, real-valued 4x4 equalizer.

B. Experimental Results with Dual Polarization Signals

In this section, the system is characterized through different P2P measurements while using SP- and DP-4QAM modulation. The Tx and Rx external LO are operated at a frequency of 8.171 GHz and 8.17 GHz with a power of approx. -9 dBm. This results in an internal LO frequency of 294.156 GHz at the Tx and an internal LO frequency of 294.12 GHz at the Rx. Both frontends are aligned at line-of-sight (LOS) and equipped with 22 dBi gain antennas. Transmission distance is 40 cm. The IF input power at the Tx frontend is varied from -13 dBm to -9 dBm in steps of 1 dB. Different symbol rates of 4, 8, 16 and 32 GBd are used. Using an RRC pulseshaping filter with roll-off factor of 0.35 (4/8/16 GBd) and 0.25 (32 GBd) results in signal bandwidths of 2.7 GHz, 5.4 GHz, 10.8 GHz and 20 GHz, respectively. The EVM is measured and evaluated to characterize the system.

Figure 5 (a) shows the constellations for H and V polarization after DSP for symbol rates of 4, 8, 16 and 32 GBd, at the maximum Tx input power of -9 dBm. It can be observed that the size of the received constellation points is increasing with the symbol rate due to the larger noise bandwidth. The shape of the received constellation points is round and well defined. Only at the symbol rate of 32 GBd, some slight deformation is visible which is attributed to nonlinearities and IQ imbalances at the Tx frontend. Furthermore, it can be noticed that the EVM can differ up to one percent between the two polarizations.

Figure 5 (b) shows the received spectra for H and V polarization at each symbol rate. The frequency response shows a decline in power towards higher frequencies, which is mainly caused by the Tx and Rx frontend properties. The maximum power at 0 GHz decreases with higher symbol rate and is attributed to wider power distribution in large spectra.

Figure 6 (a) shows the average EVM for measurements with dual polarization signals as a function of the symbol rate and the IF input power at the Tx. It can be seen that the EVM stays in a certain range, depending on symbol rate. The EVM is about 9 % to 11.4 % for a symbol rate of 4 GBd, about 11.7 % to

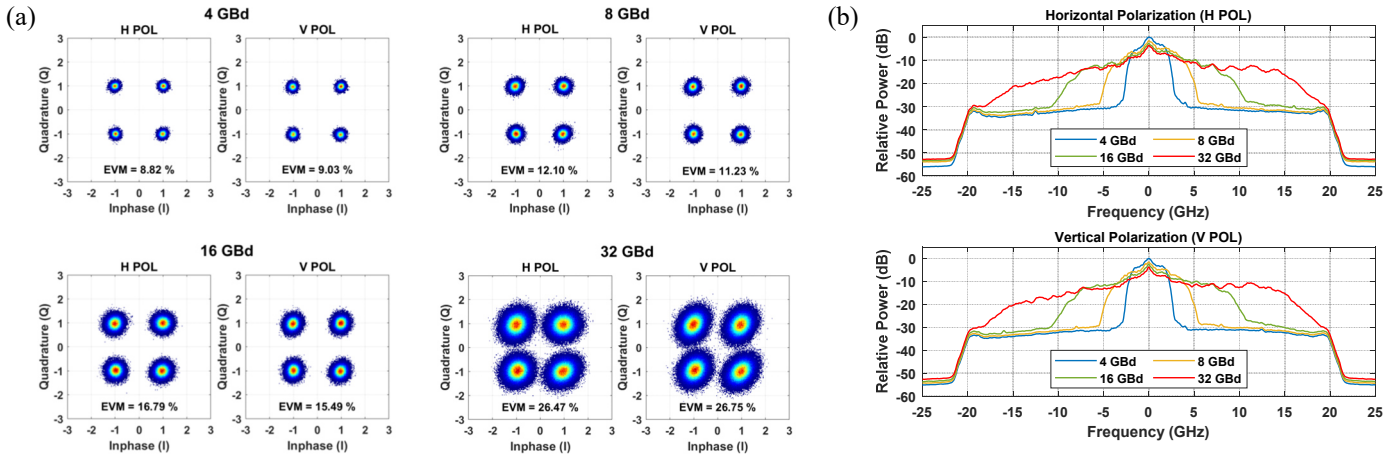

Figure 5 (a) Constellations after DSP and 4 (b) Received spectra for dual polarization with symbol rates of 4, 8, 16 and 32 GBd (Frequency resolution = 200 MHz, IF power at Tx = -9 dBm)

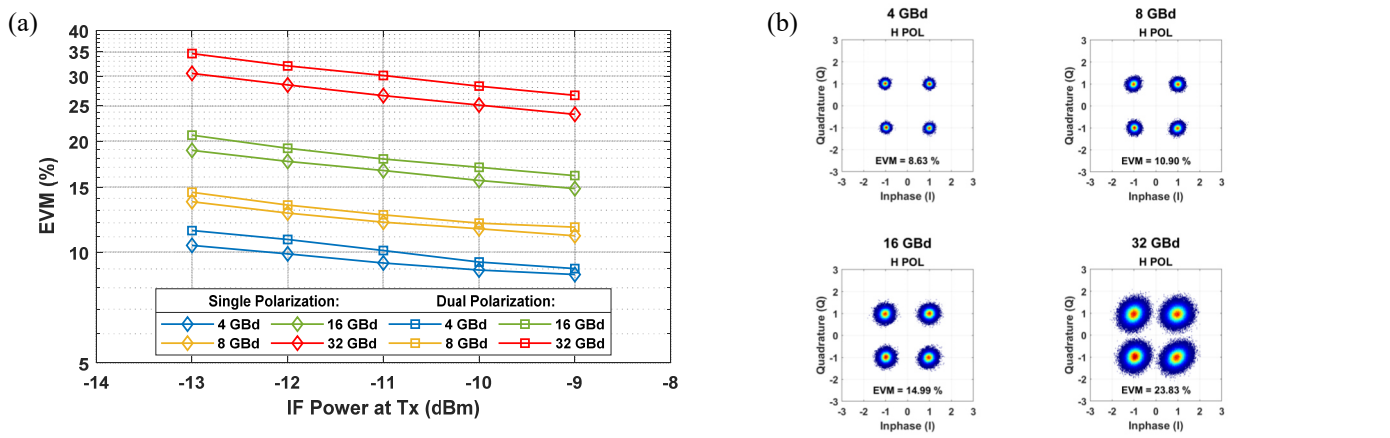

Figure 6 (a) Single Polarization and Dual Polarization EVM measurement results for symbol rates of 4, 8, 16 and 32 GBd and (b) Constellations after DSP for single polarization with symbol rates of 4, 8, 16 and 32 GBd..

14.5 % for 8 GBd, about 16.1 % to 20.8 % for 16 GBd and about 26.7 % to 34.6 % for 32 GBd. The EVM decreases with higher IF power at the Tx because of a higher received SNR at the Rx.

C. Comparison to Single Polarization Measurements

The average EVM for single polarized signals as a function of symbol rate and IF input power at the Tx is also shown in Figure 6 (a), in comparison to the results from the dual-polarization measurements. The same parameters as from the previous section are used while the Tx module is connected through only one waveguide with the OMT so that only the horizontal polarization is used.

It can be seen that the EVM stays in a certain range again but an improvement in EVM is visible for every constellation when compared to the dual polarization measurements. This is caused by the absence of polarization crosstalk. The single polarized signals EVM is improved by 0.3 % to 1 % for a symbol rate of 4 GBd, 0.6 % to 0.8 % for 8 GBd and 1.2 % to 1.9 % for 16 GBd. The highest difference of 3 % to 4 % in EVM between single and dual polarized signals can be seen at a symbol rate of 32 GBd. The constellations after DSP for single polarization with symbol rates of 4, 8, 16 and 32 GBd are shown in Figure 6 (b). The shape of the constellations is very similar to those of the dual polarization measurement but the slightly smaller distribution around the ideal constellations points can be observed.

IV. Conclusion

In this contribution, we have presented results from high-capacity dual-polarization broad-band transmission in the 300 GHz band using a new orthomode transducer with > 40 GHz bandwidth, < 3 dB linear loss and < -25 dB polarization crosstalk. We reached net bit rates of > 100 Gb/s using 4QAM modulation with symbol rates of up to 32 GBd. The comparison to single-polarization system measurements show only a small performance degradation due to polarization crosstalk.

Acknowledgment

This work has been partially funded by the German Federal Ministry of Education and Research (Bundesministerium für Bildung und Forschung, BMBF) under the AI-NET-PROTECT project with reference number 16KIS1279K and the CERTAIN project with reference number 16KIS1241K.

References

[1] I. F. Akyildiz et al., “Terahertz band: next frontier for wireless communications,” Elsevier Physical Communication, vol. 12, pp. 16-32, 2014, doi: 10.1016/J.PHYCOM.2014.01.006.

[2] A.-A. A. Boulogeourgeos et al., “Terahertz Technologies to Deliver Optical Network Quality of Experience in Wireless Systems Beyond 5G,” IEEE Communications Magazine, vol. 56, no. 6, pp. 144-151, 2018, doi: 10.1109/MCOM.2018.1700890.

[3] C. Castro et al., "Experimental Demonstrations of High-Capacity THz-Wireless Transmission Systems for Beyond 5G," IEEE Communications Magazine, vol. 58, no. 11, pp. 41-47, 2020, doi: 10.1109/MCOM.001.2000306.

[4] "IEEE Standard for High Data Rate Wireless Multi-Media Networks--Amendment 2: 100 Gb/s Wireless Switched Point-to-Point Physical Layer," IEEE Std 802.15.3d-2017 (Amendment to IEEE Std 802.15.3-2016 as amended by IEEE Std 802.15.3e-2017), 2017, doi: 10.1109/IEEESTD.2017.8066476.

[5] S. Haussmann et al., "Polarisation Multiplex in 300 GHz Wireless Communication Link using Orthomode Transducer," 2022 52nd European Microwave Conference (EuMC), 2022, pp. 776-779, doi: 10.23919/EuMC54642.2022.9924364.

[6] H. Schlegel, and W. D. Fowler, "The ortho-mode transducer offers a key to polarization diversity in EW systems", Microwave System News, September 1984, pp.65-70.

[7] A. M. Boifot, et. al., "Simple and broadband orthomode transducer", IEEE Proceedings, Vol. 137, Pt. H, No. 6, Dec 1990, pp. 396-400.

[8] A. Navarrini, and R. L. Plambeck, "A Turnstile Junction Waveguide Orthomode Transducer", IEEE Transactions on Microwave Theory and Techniques, vol. 54, no. 1, Jan. 2006 pp. 272-277.

[9] P. K. Grimes et al., "Compact broadband planar orthomode transducer," Electronic Letters, vol. 43, no. 21, pp. 1146 - 1148, 2007.

[10] G. Valente et al., "Architecture of Highly Integrated Cryogenic Active Planar OrthoMode Transducer for the 3-mm Band," 2018 2nd URSI Atlantic Radio Science Meeting (AT-RASC), 2018, pp. 1-4, doi: 10.23919/URSI-AT-RASC.2018.8471471.

[11] D. Henke and S. Claude, "Minimizing RF Performance Spikes in a Cryogenic Orthomode Transducer (OMT)," in IEEE Transactions on Microwave Theory and Techniques, vol. 62, no. 4, pp. 840-850, April 2014, doi: 10.1109/TMTT.2014.2309551.

[12] R. Elschner et al., “Experimental demonstration of a format-flexible single-carrier coherent receiver using data-aided digital signal processing,” Optics Express, vol. 20, no. 27, pp. 28786-28791, 2012, doi: 10.1364/OE.20.028786.